

1 **ONLINE SUPPLEMENT**

2

3 **Elevated Cytokine Levels in Plasma of Patients with SARS-CoV-2 do not**
4 **contribute to Pulmonary Microvascular Endothelial Permeability**

5

6

7 **Authors:** Anita Kovacs-Kasa, Abdelrahman Zaied, Silvia Leanhart, Murat Koseoglu, Supriya
8 Sridhar, Rudolf Lucas, David J. Fulton, Jose A. Vazquez, and Brian H. Annex

9

10 Methods

11 Online Figure Legends

12 Online Figures

13 References 1-14

14

15

16

17

18

19

20

21

22

23

24

25

26

27

28

29

30

31

32

33

34

35

36

37 **METHODS**

38 **Data Availability.** The authors declare that all supporting data are available within the
39 manuscript and in the Online Supplement.

40

41 Study Population

42 SARS-CoV-2 Shedding, Sequence variation, and Immune responses in confirmed and suspected
43 SARS-CoV-2 patients (SSIC Study) were approved at Augusta University Medical Center. EDTA
44 blood was collected from 8 consecutively enrolled confirmed SARS-CoV-2 positive patients on
45 the day of admission. Whole blood samples were kept on ice and plasma was separated by
46 centrifugation at $2,000 \times g$ for 5 min at 4°C (1). Plasma aliquots were stored at -80°C . In the
47 normal plasma group, we utilized commercially available pooled EDTA plasma (Innovative
48 Research, Novi, MI) and control human EDTA plasma aliquots from our plasma biobank to
49 establish a value range for the controls we used (2). 5 control plasma was used for the ECIS
50 experiments and for the cytokine profiling experiment besides the pooled plasma. Serum was
51 isolated from blood collected in serum separator tubes and stored at -80°C . Normal human serum
52 was purchased from Sigma.

53 Cell culture

54 Human Lung Microvascular ECs (HLMVECs) or human umbilical vein endothelial cells
55 (HUVECs) (Lonza, Morristown, NJ) were maintained in EBMTM-2 Basal Medium supplemented
56 with and EGMTM-2 MV Microvascular EC Growth Medium Single QuotsTM. Cells were grown at
57 37°C in a 5% CO_2 incubator and used from passage 2–6.

58 Endothelial permeability measurement with Electrical Cell Impedance Sensing System (ECIS)

59 HLMVECs were seeded on gold microelectrodes in 8 well ECIS plates (Applied Biophysics, Troy,
60 NY) as it was described previously (3). Briefly, EC monolayers resistance was tested by measuring
61 transendothelial resistance (TER) in real-time. After the baseline was set, cells were challenged
62 either with normal pooled plasma or SARS-CoV-2 patient's plasma (1:200) in EGM-2, and TER
63 was monitored for 15-20 hours in the presence of plasma or other treatments. IL-6, IL-10, IL-17,
64 IFN- γ , ACE-2 neutralizing antibodies, soluble TNF receptor were used as a 2h pretreatment before
65 plasma treatment. Recombinant SARS-CoV-2 Spike Protein, S1 Subunit, and Host Cell Receptor
66 Binding Domain (RBD) were purchased from Ray Biotech (Atlanta, GA).

67 Immunostaining

68 Human Lung ECs were grown to confluence on glass coverslips. HLMVEC were treated with
69 plasma from SARS-CoV-2 patients for 1 hr. Then EC monolayers were washed with 1xPBS twice,
70 then fixed with 3.7% paraformaldehyde (PFA) for 10 minutes on RT. After 5 min RT
71 permeabilization (0.25% Triton X-100 in Tris-buffered saline with 0.1% Tween) HLMVECs were
72 blocked with 2% bovine serum albumin in TBST for 1hr. Primary antibodies were added overnight
73 1:500 dilution. Secondary antibody in 1:300 was incubated with the cells for 1 hr. between each
74 step, cells were rinsed three times with 1 \times PBS. Coverslips were rinsed with 1xPBS, then mounted
75 with ProLong[®] Gold Antifade Reagent and observed with \times 40 immersion oil objective lenses
76 using a Zeiss 780 Upright Confocal microscope at Augusta University Core Lab.

77 Image Analysis

78 The Gap area on an endothelial monolayer of CD31, VE-Cadherin, and F-actin was analyzed using
79 ImageJ & Fiji software. The area of interendothelial gaps was outlined manually. The values were
80 expressed as a percentile of the total surface area. Mean fluorescence intensity was analyzed by

81 ZEN Blue software by selecting the same size area on the normal plasma or SARS-CoV-2 plasma-
82 treated images. Images were thresholded by subtracting the background.

83 Cytokine assay

84 A panel of 15 pro-and anti-inflammatory cytokines; interleukin (Il)1 beta (IL-1 β), IL-2, IL-4, IL-
85 6, IL-7, IL-8, IL-10, IL-12p70, IL-13, IL-17A, IL-21, macrophage inflammatory protein-1 alpha
86 (MIP1 α), interferon-gamma (IFN γ), TNF- α , and granulocyte-macrophage colony-stimulating
87 factor (GM-CSF) was assessed in duplicates in 50 μ L plasma from the study subjects, using a
88 highly sensitive cytokine bead assay (MILLIPLEX MAP High Sensitivity Human Cytokine Panel
89 – Premixed 13 Plex, EMD Millipore (4, 5)).

90 ELISA

91 Human VEGF or Ang2 Quantikine ELISA Kit (R&D Systems, Minneapolis, MN) or COVID-19,
92 Spike Protein ELISA Kit (Abcam Cambridge, MA) were used to measure levels of VEGF and
93 Ang2 in SARS-CoV-2 patient plasma or levels of spike protein in SARS-CoV-2 patients' sera. In
94 total, 100 μ L of each standard and sample (1:20) were added into appropriate wells and incubated
95 for 2.5 hours at room temperature. After discarding the solution the plate was washed 4 times with
96 1X Wash Solution. 100 μ L of 1X Biotinylated Angiopoietin 2 Detection Antibody was added to
97 each well, then incubated for 1 hour at RT. After washing 100 μ L of 1X HRP-Streptavidin solution
98 was added to the wells and incubated for 45 minutes at RT. 100 μ L of TMB One-Step Substrate
99 Reagent was added to the wells for 30 minutes at RT in the dark. After the addition of 50 μ L of
100 Stop Solution, absorbance was read at 450 nm.

101 Cell viability

102 Human lung microvascular ECs plated in 96 well plate were either treated with normal pooled
103 plasma (1:200 dilution) or SARS-CoV-2 patients' plasma (1:200 dilution) for 1 hr. Then highly

104 water-soluble tetrazolium salt, WST-8 was added to the cells and further incubated for 1 hour. Cell
105 viability was assessed by reading the absorbance at 450nm.

106 Statistical analysis

107 Independent experiments were performed at least three times to allow statistical analysis.
108 Normality was evaluated using the Shapiro–Wilk test and statistical significance was assessed by
109 one-way ANOVA followed by Tukey’s post hoc test to analyze the difference between three or
110 more groups. Dunnett's post hoc test was used for multiple comparisons using Graph Pad Prism.
111 Results are presented as mean \pm SEM and differences were considered statistically significant at p
112 values ≤ 0.05 .

113

114

115

116

117

118

119

120

121

122

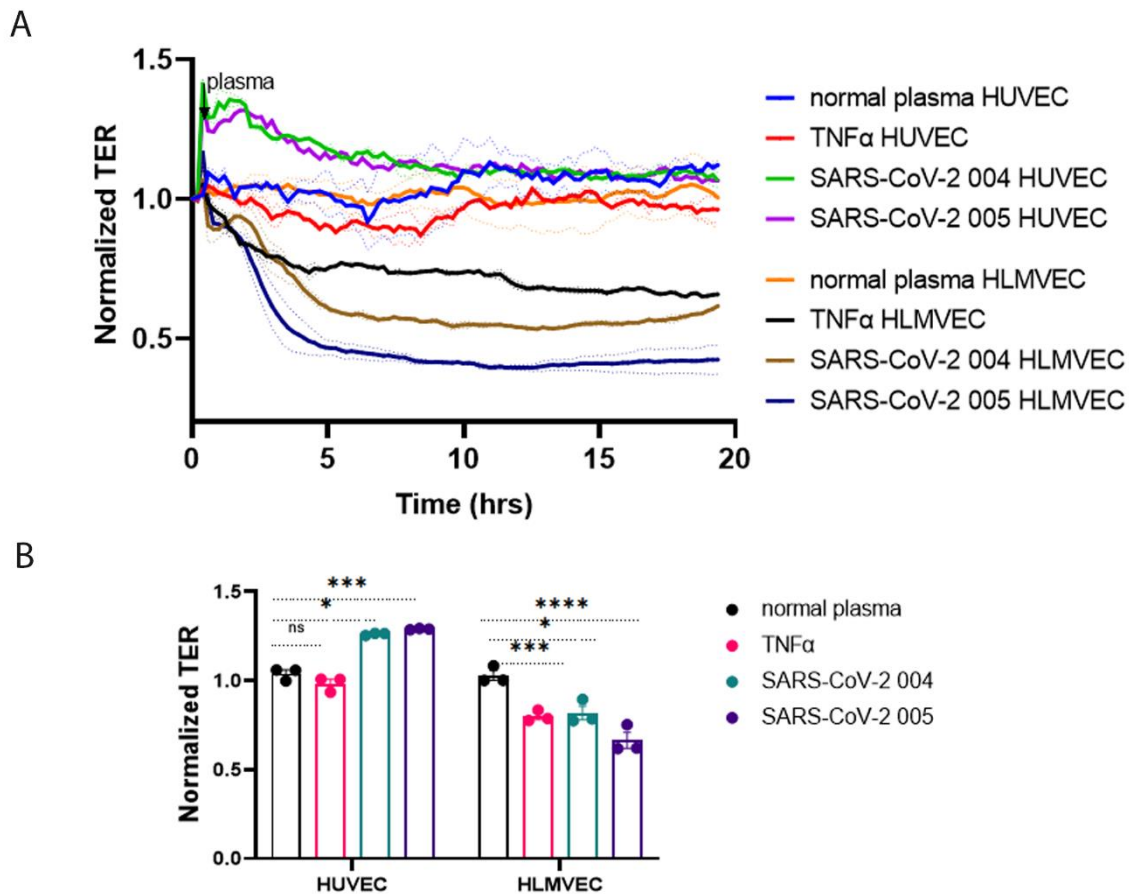
123

124

125

126

Supplementary Figure 1

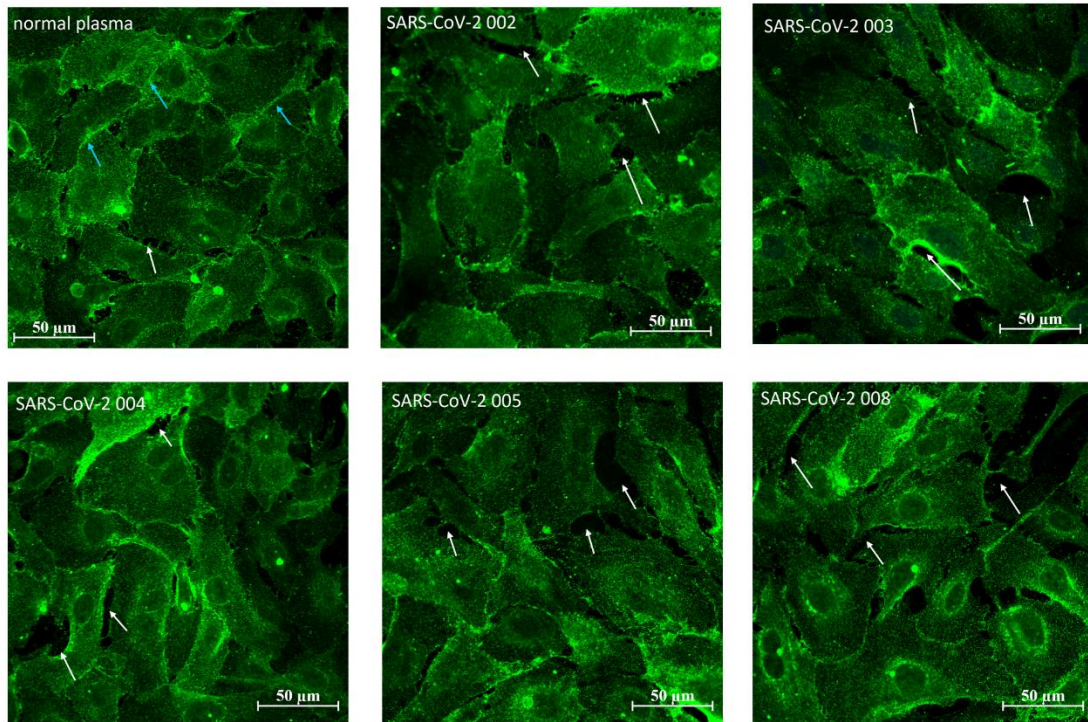


128 **Figure S1. SARS-CoV-2 patient plasma does not alter endothelial permeability in human**
 129 **umbilical vein endothelial cells.** A. HUVECs or HLMVEC were plated in ECIS arrays, a baseline
 130 was set, then cells were challenged either with normal or SARS-CoV-2 patient plasma (004 and
 131 005) or with TNF α (1 ng/ml) and TER was monitored for 20 hours. Cells were treated at the 0-
 132 time point. B. Bar graph represents side by side resistance values of HUVEC and HLMVEC for
 133 normal plasma, SARS-CoV-2 plasma, and TNF α . Representative graph is shown from three
 134 independent experiments, n=3 in each group. *p < 0.05 normal plasma vs. SARS-CoV-2 004 in
 135 both HUVECs and HLMVECs, ***p=0.0001 normal plasma vs. SARS-CoV-2 005 in HUVECs

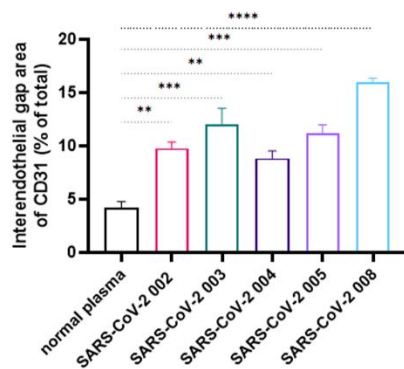
136 and normal plasma vs. TNF α in HLMVEC, ****p < 0.0001 normal plasma vs. SARS-CoV-2 005
 137 in HLMVECs. The statistical significance was assessed by one-way ANOVA followed by Tukey's
 138 multiple comparisons post hoc test using Graph Pad Prism.
 139

Supplementary Figure 2

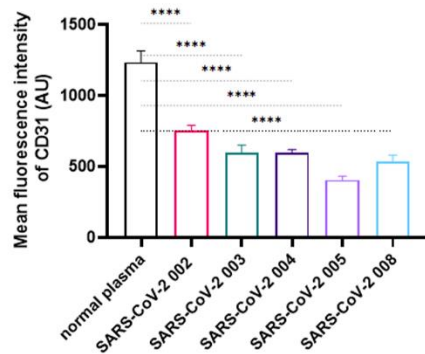
A



B



C

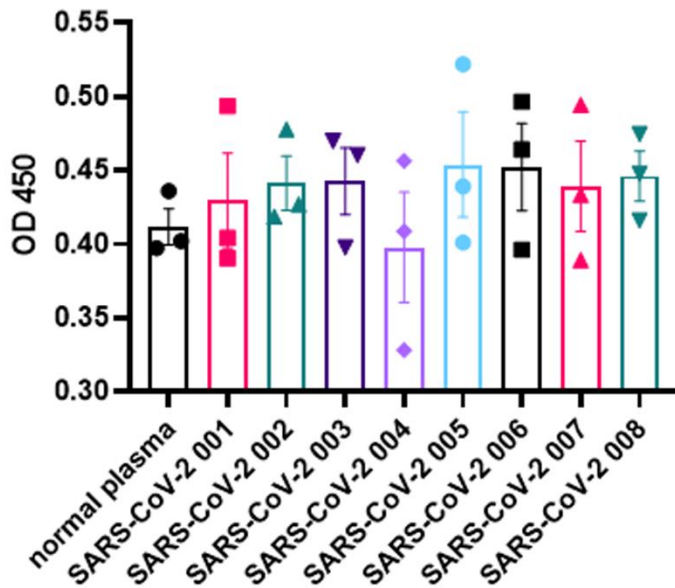


140

141 **Figure S2. Impaired EC barrier after SARS-CoV-2 plasma treatment showed by CD31**
 142 **staining.** HLMVEC were treated either with normal pooled plasma (A) or with SARS-CoV-2
 143 plasma in (1:200) 1 hour. Then cells were stained for CD31. Images were captured by Zeiss 780
 144 Upright Confocal microscope, using 40x Plan-Apo (oil) objective. Scale bar is 50 μ M. (B) Bar
 145 graph represents mean \pm SEM of gap area on HLMVEC monolayers, expressed as a percent of the
 146 total area of each image treated either with normal or SARS-CoV-2 plasma (n=3). (C) Bar graphs
 147 represent mean \pm SEM of fluorescence intensity of CD31 on HLMVEC monolayers treated either
 148 with normal or SARS-CoV-2 plasma (n=5). **p < 0.01, ***p = 0.0001, ****p < 0.0001 vs. normal
 149 plasma. The statistical significance was assessed by one-way ANOVA followed by Tukey's
 150 multiple comparisons post hoc test using Graph Pad Prism.

151

Supplementary Figure 3

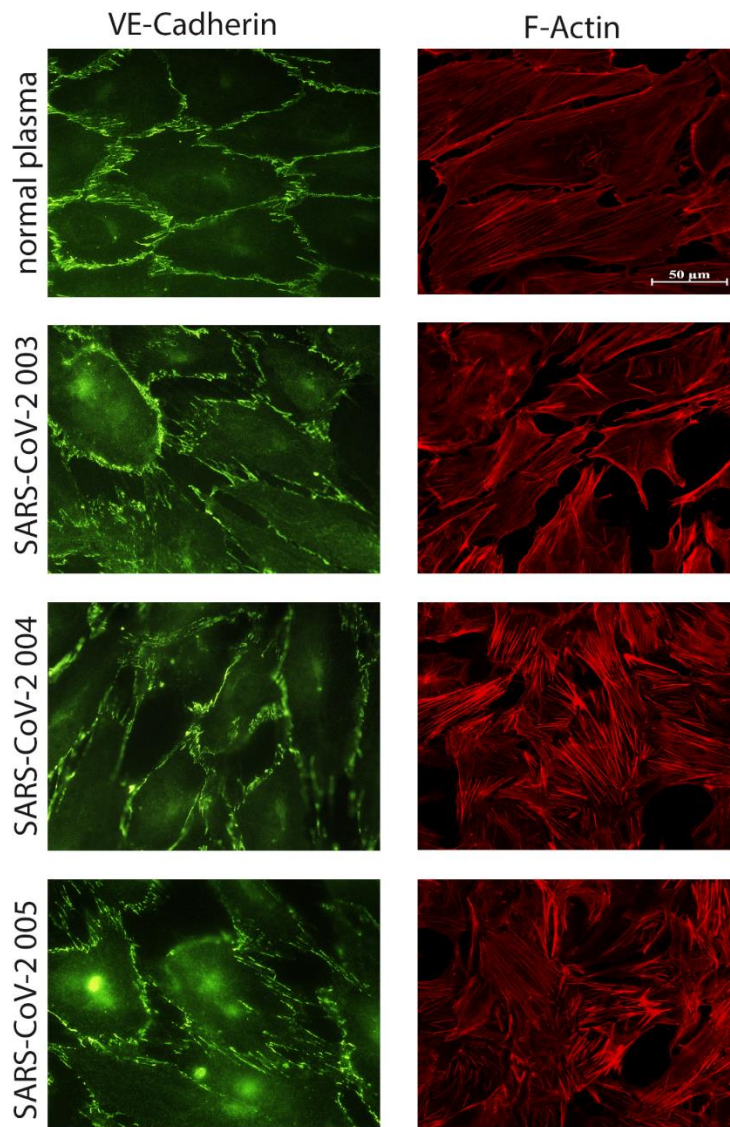


152

153 **Figure S3. SARS-CoV-2 plasma has no effect on cell viability.** HLMVEC were treated either
154 with normal pooled plasma or with SARS-CoV-2 plasma in 1:200 dilution in normal growth media
155 for 1 hours. Water soluble tetrazolium (WST8) was added to the cells in cell survival proliferation
156 assay at 1 hours after the plasma addition. Absorbance was measured at 450 nm. Representative
157 data of 3 experiments .Values are present as Mean±SEM, n=8/group.
158

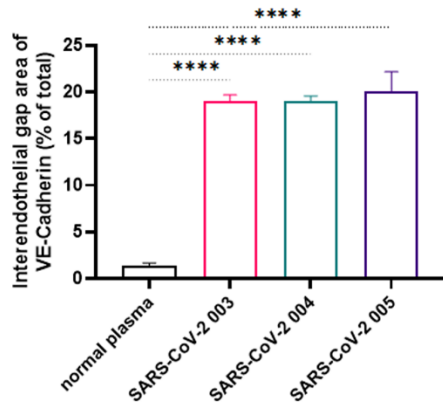
Supplementary Figure 4

A

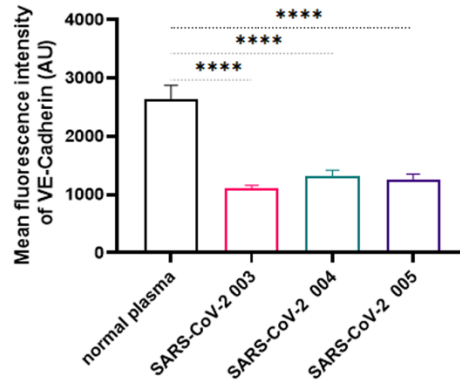


Supplementary Figure 4

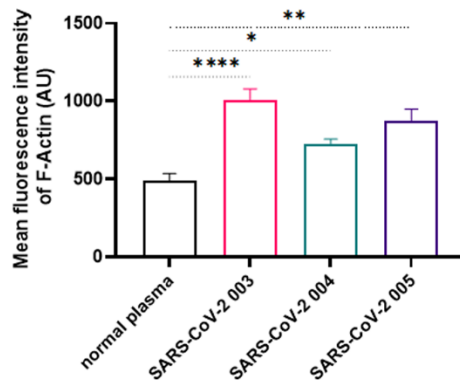
B



C



D



161

162 **Figure S4. Disruption in Adherens Junctions and cytoskeletal rearrangement after SARS-**

163 **CoV-2 plasma treatment.** HLMVEC were treated either with normal pooled plasma (A) or with

164 SARS-CoV-2 plasma in 1:200 dilution in normal growth media for 1 hour. Then cells were stained

165 for VE-Cadherin or F-Actin by immunofluorescence. Images were captured by Zeiss 780 Upright

166 Confocal microscope, using 40x Plan-Apo (oil) objective. (B) Bar graph represents mean \pm SEM

167 of gap area on HLMVEC monolayers, expressed as a percent of the total area of each image treated

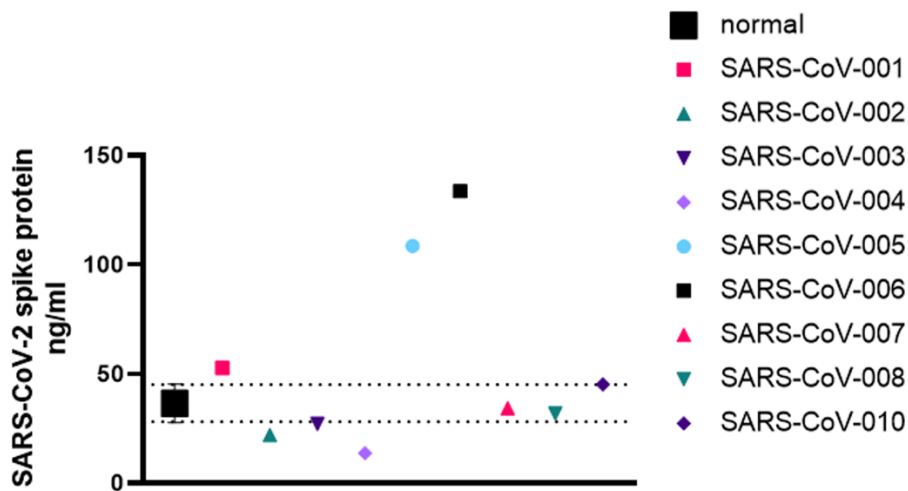
168 either with normal or SARS-CoV-2 plasma (n=3). (C) Bar graphs represent mean \pm SEM of

169 fluorescence intensity of VE-Cadherin on HLMVEC monolayers treated either with normal or

170 SARS-CoV-2 plasma (n=5). (D) Bar graphs represent mean \pm SEM of fluorescence intensity of F-

171 Actin on HLMVEC monolayers treated either with normal or SARS-CoV-2 plasma (n=5). Scale
172 bar is 50 μ M. Images were analyzed by the ZEN blue program. * $p < 0.05$, ** $p < 0.01$,
173 **** $p < 0.0001$ vs. normal plasma. The statistical significance was assessed by one-way ANOVA
174 followed by Tukey's multiple comparisons post hoc test using Graph Pad Prism.

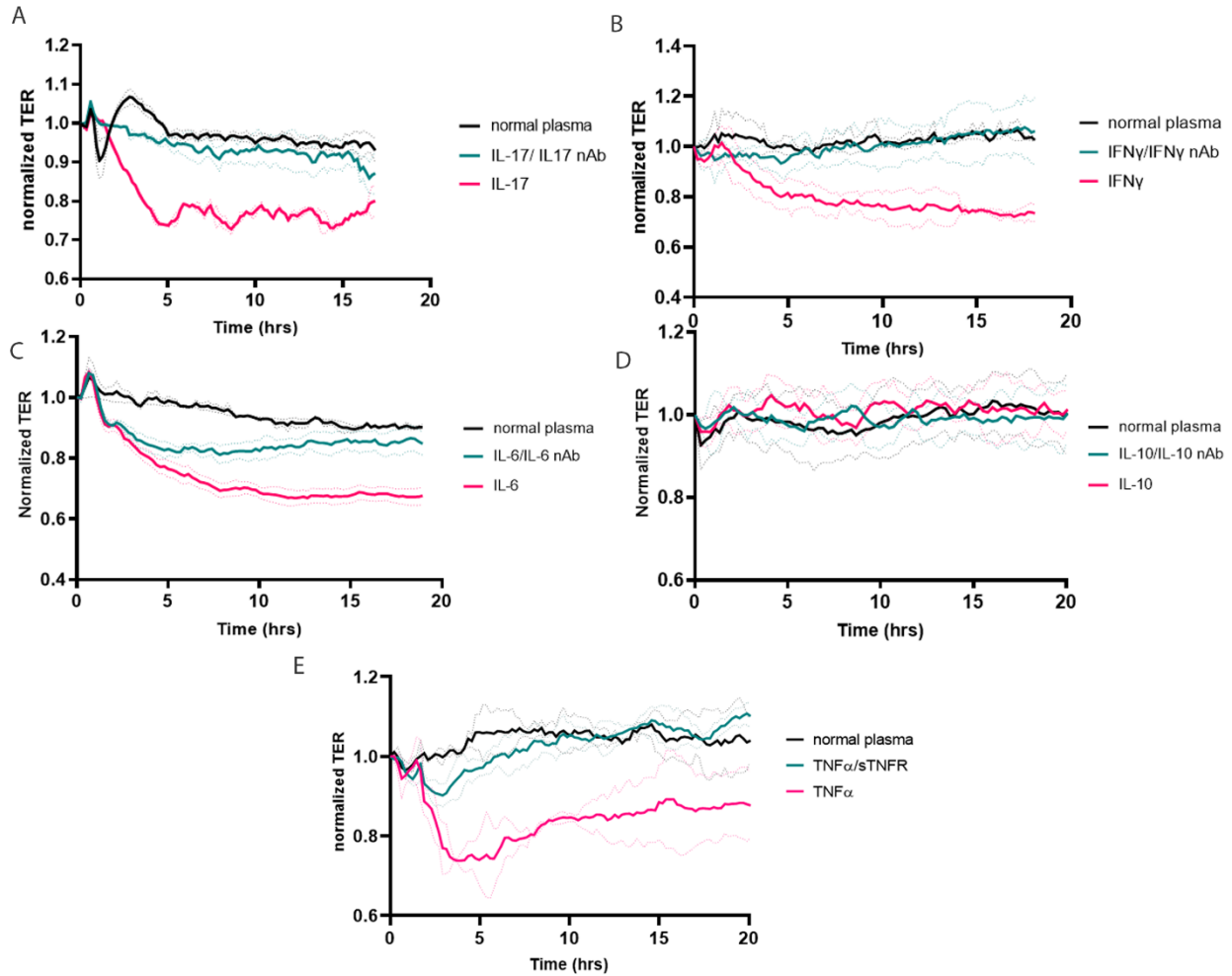
Supplementary Figure 5



175
176 **Figure S5. Spike protein concentration is not elevated in SARS-CoV-2 patients' samples.**
177 Spike protein concentrations were measured from SARS-CoV-2 patients' sera and compared to
178 normal human serum (Sigma) using COVID-19 Spike Protein ELISA Kit (Abcam). OD values
179 were measured at 450 nm. The dashed line shows the level of the SARS-CoV-2 spike protein in
180 the normal plasma samples. Values are present as Mean \pm SEM.

181

Supplementary Figure 6



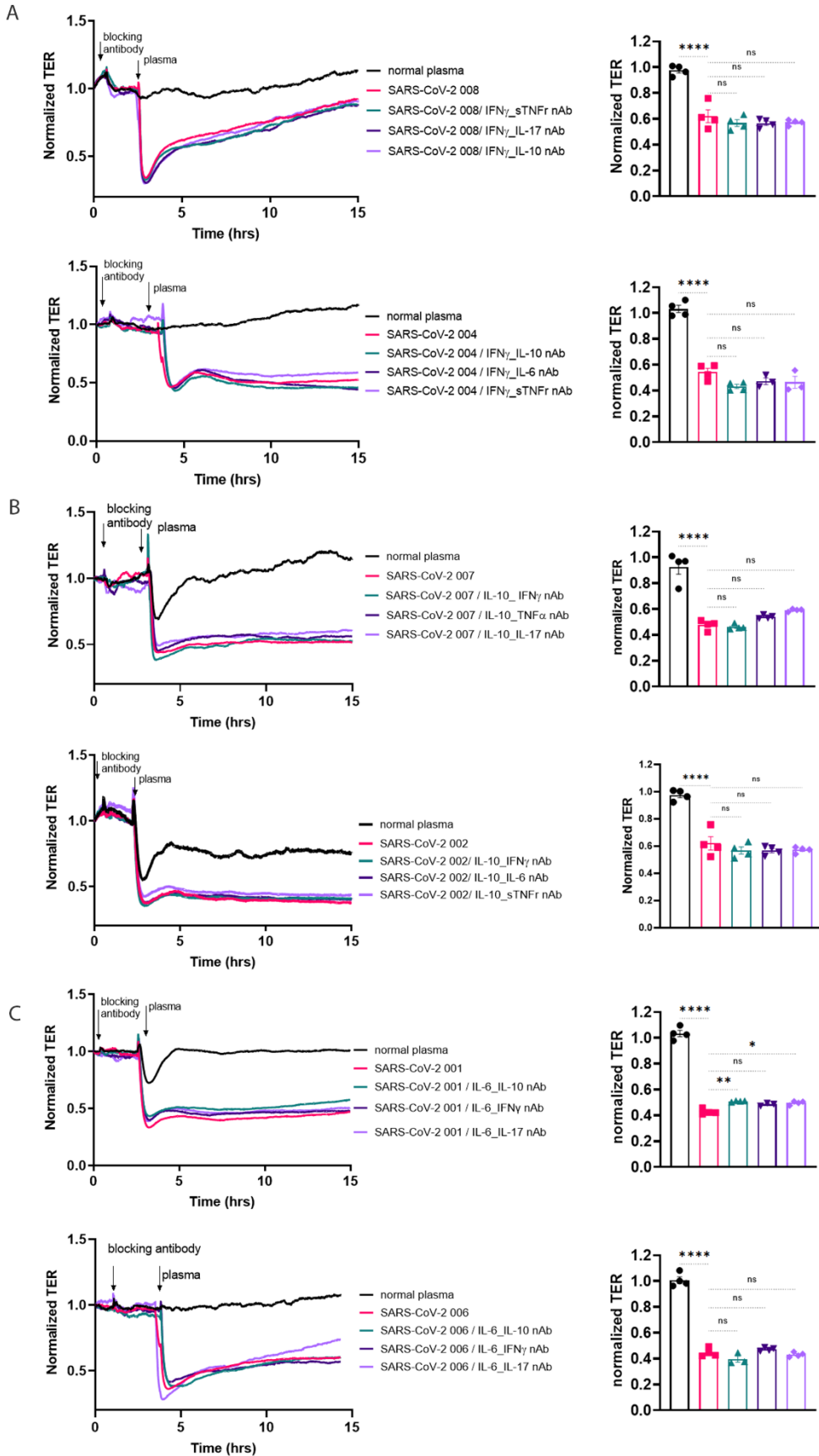
182

183 **Figure S6. Effect of IL-17, IFN γ , IL-6, IL-10, and TNF α effect on endothelial permeability.**

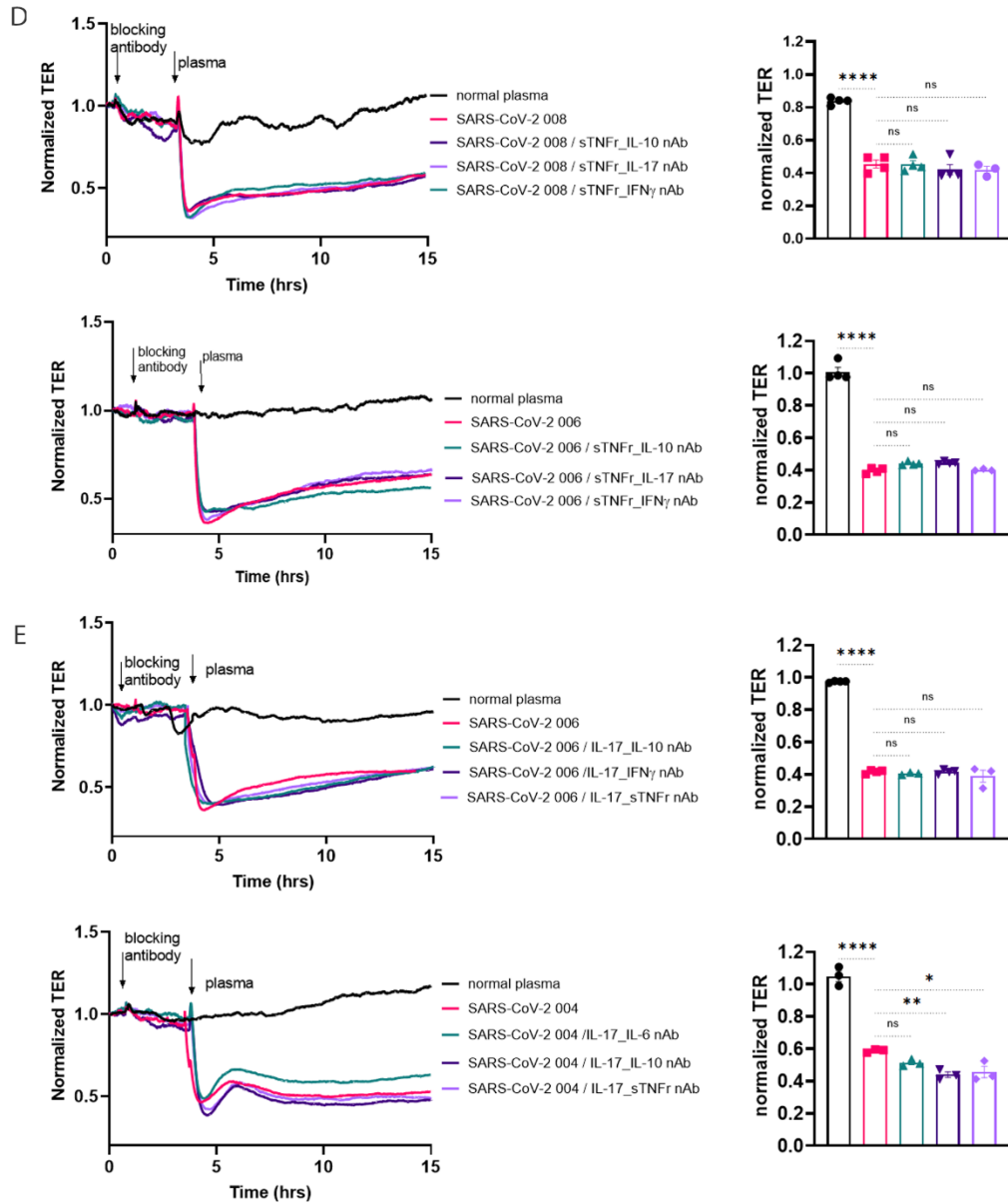
184 We tested the effect of A) IL-17 (1 ng/ml) with or without IL-17 neutralizing antibody (nAb) (5
185 ng/ml), B) IFN γ (1 ng/ml) with or without IFN γ nAb (1 ng/ml), C) IL-6 (20 ng/ml) with or without
186 IL-6 nAb (5 ng/ml), and D) IL-10 (10 ng/ml) with or without IL-10 nAb (25 ng/ml) E) TNF α (1
187 ng/ml) with or without the soluble TNF receptor (1 ng/ml) on endothelial permeability. TER was
188 monitored for 18-20 hours. Commercially available pooled normal human plasma was used as the
189 normal plasma group control. Results are shown from 3 independent experiments, n=3.

190

Supplementary Figure 7



Supplementary Figure 7



206 **Figure S7. Combined blocking antibody combinations fail to reduce endothelial injury after**
 207 **exposure to SARS-CoV-2 plasma.** HLMVECs monolayers were incubated with combinations of
 208 the indicated blocking antibodies for two hours prior to exposure to SARS-CoV-2 plasma (1:200
 209 dilution in normal growth media) and TER was monitored for 18 hours. For each of the cytokines
 210 individually targeted in Figure 3 including IFN γ , IL-10, TNF α , IL-6, and IL-17. For each cytokine

211 target, 1 patient plasma with the second-highest fold increase and 1 patient plasma with the lowest
 212 or no increase was selected for the double targeting. (A) SARS-CoV-2 patient 008 and 004; B)
 213 SARS-CoV-2 patient 007 and 002; C) SARS-CoV-2 patient 001 and 006; D) SARS-CoV-2 patient
 214 008 and 006; E) SARS-CoV-2 patient 006 and 004. For each of these selected patient plasma, the
 215 three other indicated cytokines with the highest increase were selected as the second target. Arrows
 216 indicate the treatment time points. Bar graphs represent the selected time points for statistical
 217 analysis to compare each treatment group at 2 hours after SARS-CoV-2 plasma treatment. Results
 218 are expressed as Mean \pm SEM of 3 independent experiments, n=5. *p < 0.05, **p < 0.01,
 219 ****p < 0.0001 vs. normal plasma. The statistical significance was assessed by one-way ANOVA
 220 followed by Tukey's multiple comparisons post hoc test using Graph Pad Prism.

221 **Supplementary Tables**

222 Table S1. SARS-CoV-2 patient's characteristics.

SARS-CoV-2 patient	Sex	Age	Intubated day of admission	Intubated during clinical course	ICU Admission ²²³
001	F	69	N	Y	Y ²²⁵
002	F	78	N	N	N
003	M	41	N	Y	Y ²²⁶
004	F	70	N	N	N
005	F	76	N	N	Y ²²⁷
006	F	29	N	N	N
007	M	20	N	N	N ²²⁸
008	F	73	N	N	Y ²²⁹

230
 231
 232
 233

234 Table S2. Pro-inflammatory cytokines involved in vascular permeability.

cytokine	Levels in SARS-CoV-2 (total of 8 patients)	Effect on EC barrier	References
IL-10	↑ in 8 patients	Inhibits vascular leakage	(6)
IL-6	↑ in 7 patients	Promotes loss of endothelial barrier function	(7, 8)
IFN γ	↑ in 7 patients	Increase vascular permeability	(9, 10)
TNF α	↑ in 6 patients	Disrupt EC barrier function	(11, 12)
IL-17A	↑ in 5 patients	Break down blood brain barrier	(13, 14)

235

236 Table S3. Neutralizing antibody combinations for each cytokine in 3 selected patients.

Interferon γ			
SARS-CoV-2 patient	cytokine fold change	blocking antibody combinations	fold changes of 2nd cytokine target
	increased	IFN γ / IL-10	25
SARS-CoV-2 006	3	IFN γ / IL-17	3
		IFN γ / sTNFr	1
	increased	IFN γ / sTNFr	2
SARS-CoV-2 008	3	IFN γ / IL-17	3
		IFN γ / IL-10	26
	no change	IFN γ / IL-10	21
SARS-CoV-2 004	0	IFN γ / IL-6	4
		IFN γ / sTNFr	2

237

Interleukin-10			
SARS-CoV-2 patient	Cytokine fold change	blocking antibody combinations	fold changes of 2nd cytokine target
	increased	IL-10 / IL-6	8
SARS-CoV-2 001	63	IL-10 / IFN γ	2
		IL-10 / IL-17	2
	increased	IL-10 / IFN γ	2
SARS-CoV-2 007	37	IL-10 / sTNFr	2
		IL-10 / IL-17	2
	increased	IL-10 / IL-6	7
SARS-CoV-2 002	11	IL-10 / IFN γ	2
		IL-10 / sTNFr	2

238

239

Tumor Necrosis Factor α			
SARS-CoV-2 patient	cytokine fold change	blocking antibody combinations	fold changes of 2nd cytokine target
	increased	sTNFr / IFN γ	3
SARS-CoV-2 008	2	sTNFr / IL-10	26
		sTNFr / IL-17	3
	increased	sTNFr / IL-10	22
SARS-CoV-2 005	2	sTNFr / IL-6	4
		sTNFr / IFN γ	1
	increased	sTNFr / IL-10	25
SARS-CoV-2 006	0.6	sTNFr / IL-17	4
		sTNFr / IL-IFN γ	6

240

241

242

Interleukin-6			
SARS-CoV-2 patient	cytokine fold change	blocking antibody combinations	fold changes of 2nd cytokine target
	increased	IL-6 / IL-10	63
SARS-CoV-2 001	8	IL-6 / IFN γ	2
		IL-6 / IL-17	2
	increased	IL-6 / IL-10	11
SARS-CoV-2 002	7	IL-6 / IFN γ	2
		IL-6 / sTNFr	2
	increased	IL-6 / IL-10	25
SARS-CoV-2 006	1	IL-6 / IFN γ	3
		IL-6 / IL-17	3

243

Interleukin-17			
SARS-CoV-2 patient	cytokine fold change	blocking antibody combinations	fold changes of 2nd cytokine target
	increased	IL-17 / sTNFr	2
SARS-CoV-2 008	3	IL-17 / IFN γ	3
		IL-17 / IL-10	26
	increased	IL-17 / IL-10	25
SARS-CoV-2 006	3	IL-17 / IFN γ	3
		IL-17 / sTNFr	1
	increased	IL-17 / IL-6	4
SARS-CoV-2 004	1	IL-17 / IL-10	21
		IL-17 / sTNFr	3

244

245

246

247

248

249

250 **References**

251

252

- 253 1. Findley CM, Mitchell RG, Duscha BD, Annex BH, Kontos CD. 2008. Plasma levels of soluble Tie2
254 and vascular endothelial growth factor distinguish critical limb ischemia from intermittent
255 claudication in patients with peripheral arterial disease. *J Am Coll Cardiol* 52:387-93.
- 256 2. Ganta VC, Choi M, Farber CR, Annex BH. 2019. Antiangiogenic VEGF165b Regulates Macrophage
257 Polarization via S100A8/S100A9 in Peripheral Artery Disease. *Circulation* 139:226-242.
- 258 3. Kovacs-Kasa A, Varn MN, Verin AD, Gonzales JN. 2017. Method for the Culture of Mouse
259 Pulmonary Microvascular Endothelial Cells. *Sci Pages Pulmonol* 1:7-18.
- 260 4. Elshal MF, McCoy JP. 2006. Multiplex bead array assays: performance evaluation and
261 comparison of sensitivity to ELISA. *Methods* 38:317-23.
- 262 5. Richens JL, Urbanowicz RA, Metcalf R, Corne J, O'Shea P, Fairclough L. 2010. Quantitative
263 validation and comparison of multiplex cytokine kits. *J Biomol Screen* 15:562-8.
- 264 6. Li L, Elliott JF, Mosmann TR. 1994. IL-10 inhibits cytokine production, vascular leakage, and
265 swelling during T helper 1 cell-induced delayed-type hypersensitivity. *J Immunol* 153:3967-78.
- 266 7. Alsaffar H, Martino N, Garrett JP, Adam AP. 2018. Interleukin-6 promotes a sustained loss of
267 endothelial barrier function via Janus kinase-mediated STAT3 phosphorylation and de novo
268 protein synthesis. *Am J Physiol Cell Physiol* 314:C589-C602.
- 269 8. Blecharz-Lang KG, Wagner J, Fries A, Nieminen-Kelha M, Rosner J, Schneider UC, Vajkoczy P.
270 2018. Interleukin 6-Mediated Endothelial Barrier Disturbances Can Be Attenuated by Blockade
271 of the IL6 Receptor Expressed in Brain Microvascular Endothelial Cells. *Transl Stroke Res* 9:631-
272 642.
- 273 9. Stewart RJ, Kashour TS, Marsden PA. 1996. Vascular endothelial platelet endothelial adhesion
274 molecule-1 (PECAM-1) expression is decreased by TNF-alpha and IFN-gamma. Evidence for
275 cytokine-induced destabilization of messenger ribonucleic acid transcripts in bovine endothelial
276 cells. *J Immunol* 156:1221-8.
- 277 10. Youakim A, Ahdieh M. 1999. Interferon-gamma decreases barrier function in T84 cells by
278 reducing ZO-1 levels and disrupting apical actin. *Am J Physiol* 276:G1279-88.
- 279 11. Clark PR, Kim RK, Pober JS, Kluger MS. 2015. Tumor necrosis factor disrupts claudin-5
280 endothelial tight junction barriers in two distinct NF-kappaB-dependent phases. *PLoS One*
281 10:e0120075.
- 282 12. Adam AP, Lowery AM, Martino N, Alsaffar H, Vincent PA. 2016. Src Family Kinases Modulate the
283 Loss of Endothelial Barrier Function in Response to TNF-alpha: Crosstalk with p38 Signaling. *PLoS*
284 *One* 11:e0161975.
- 285 13. Zenobia C, Hajishengallis G. 2015. Basic biology and role of interleukin-17 in immunity and
286 inflammation. *Periodontol* 2000 69:142-59.
- 287 14. McGinley AM, Sutton CE, Edwards SC, Leane CM, DeCoursey J, Teijeiro A, Hamilton JA, Boon L,
288 Djouder N, Mills KHG. 2020. Interleukin-17A Serves a Priming Role in Autoimmunity by
289 Recruiting IL-1beta-Producing Myeloid Cells that Promote Pathogenic T Cells. *Immunity* 52:342-
290 356 e6.

291